Journal of Drug Delivery Science and Technology 50 (2019) 329–338

Contents lists available at ScienceDirect

Journal of Drug Delivery Science and Technology

journal homepage: www.elsevier.com/locate/jddst

Chamomile oil loaded solid lipid nanoparticles: A naturally formulated remedy to enhance the wound healing

Heba A. Gad[a,*], Fawzia A.A. Abd El-Rahman[b], Germine M. Hamdy[c]

[a] Department of Pharmaceutics and Industrial Pharmacy, Faculty of Pharmacy, Ain Shams University, Cairo, Egypt
[b] Zoology Department, Faculty of Science, Ain Shams University, Cairo, Egypt
[c] Biochemistry Department, Faculty of Science, Ain Shams University, Cairo, Egypt

ARTICLE INFO

Keywords:
Chamomile oil
Solid lipid nanoparticles
Wound healing
Inflammatory mediators
Skin histopathology

ABSTRACT

Chamomile oil (CM) has a crucial effect in promoting wound healing, but its poor tissue permeability and degradation limit its topical application. The aim of the present study is to ameliorate CM healing effect by encapsulating it into solid lipid nanoparticles (SLN). SLN were prepared by hot homogenization method using 20%w/w stearic acid and CM. The *in-vivo* study involved 40 rats divided into 5 groups. Group I: was normal control, Group II: represented wounded rats without treatment and Groups III to V: were wounded rats treated with plain SLN, CM cream (Camisan®) and CM-SLN, respectively. Morphological examination of CM loaded SLN revealed irregular shaped particles with an outer chamomile oil shell surrounding the lipid core. Optimized CM-SLN formed of stearic acid and CM (in ratio 7:3) had particle size of 542.1 ± 27.51 nm and zeta potential of −35.9 ± 0.602 mV with acceptable viscosity and occlusive properties. Topical administration of CM-SLN showed improvement in restoring the normal integument architecture, wound contraction, transforming growth factor-β1 and collagen deposition, in addition to the reduction in the Interleulin-1β and metalloproteinases-9/tissue inhibitor metalloproteinase-1 ratio, as compared to the other groups. In conclusion, the encapsulation of CM in SLN showed a significant effect in accelerating the wound healing activity.

1. Introduction

Wound healing or normal tissue repair is a highly regulated cascade of multiple cellular and molecular processes. It consists of four main phases of hemostasis, inflammation, proliferation and tissue remolding that occur in an integrated sequencing manner [1]. Various cell types such as platelets, neutrophils, macrophages, and fibroblasts play a vital role in the healing process. The neutrophils remove bacteria and damaged debris by phagocytosis, followed by the release of many cytokines by the macrophages. The released cytokines include interleukins (ILs) and signal growth factors such as transforming growth factors–-beta (TGF-B). During the proliferative phase, TGF- β1 plays a crucial role in enhancing the wound closure and is involved in all phases of healing process. It improves the angiogenic properties of endothelial cells and modulates the cell proliferation, in addition to its stimulating effect on the fibroblast contraction [2]. Fibroblasts, in turn, accelerate the extracellular matrix molecules (ECM) laying, in which collagen-1 represents its main component and is responsible for the structural strength and integrity in tissues. Collagen stimulates many crucial processes in the wound healing including; angiogenesis, epithelialization, proliferation, and tissue remolding [3].

Simultaneously, many white cells and connective tissue cells stimulate the secretion of both the specific matrix metalloproteinases (MMP) enzymes and their tissue inhibitors (TIMPs). Matrix metalloprotenaises levels are down regulated in normal skin, while wounding strongly induces their expression and hence their activity levels [4]. Their main function is degrading and destroying the irregular portions of the extracellular matrix protein, leading to the granulation tissue remodeling, re-epithelization and angiogenesis modulation [5].

Unfortunately, disruption or falling in one of these complex molecular or cellular processes impairs the ability of the wound to heal normally. These impaired wound healing enter a state of pathologic inflammation accompanied with high levels of interleukins especially IL-1 and IL-6 [6], poor response of fibroblasts to any inflammatory stimuli as well as a decline in the growth factors levels especially TGF-β1 [2]. At the same time, chronic or non-healing wounds show slow collagen synthesis, increased MMPs activity and abnormally high MMP/TIMP ratio, leading to ECM degradation as well as impaired

* Corresponding author. Department of Pharmaceutics and Industrial Pharmacy, Faculty of Pharmacy, Ain Shams University, Organization of African unity Street, 11566-Abbasseya, Cairo, Egypt.
E-mail address: h.gad@pharma.asu.edu.eg (H.A. Gad).

https://doi.org/10.1016/j.jddst.2019.01.008
Received 3 October 2018; Received in revised form 31 December 2018; Accepted 8 January 2019
Available online 09 January 2019
1773-2247/ © 2019 Elsevier B.V. All rights reserved.

Table 1
Composition and characterization of chamomile oil loaded solid lipid nanoparticles.

Formula	SA:CM	Particle size (nm) ± S.D.	PDI ± S.D.	Zeta potential (mV) ± S.D.	Occlusion Factor ± S.D.	Viscosity (Pa.s) ± S.D.
F1	10:0	619.0 ± 9.758	0.347 ± 0.040	−27.5 ± 0.707	56.41 ± 3.74	5.80 ± 1.22
F2	9:1	572.8 ± 6.285	0.273 ± 0.029	−34.5 ± 0.245	46.15 ± 0.17	4.10 ± 2.20
F3	7:3	542.1 ± 27.51	0.353 ± 0.016	−35.9 ± 0.602	43.58 ± 1.87	3.14 ± 0.75
F4	1:1	956.5 ± 67.70	0.723 ± 0.072	−29.9 ± 0.495	38.46 ± 1.21	1.70 ± 0.05

SA: Stearic acid, CM: Chamomile, PDI: polydispersity index, S.D.: standard deviation.

angiogenesis [7].

Chronic or non-healing wounds represent a silent epidemic problem, producing high economic load on the society and resulting in enormous morbidity and mortality for a large portion of the world population [8]. Therefore, some pharmaceutical and biomedical researchers focused their attention on the use of essential oils as a topical wound healing treatment due to their safety, lower cost as well as their potential efficacy [9].

Chamomile oil (CM) is one of the most commonly used herbs owing to its anti-inflammatory, antibacterial, antioxidant and anti-irritant activities, in addition to its good occlusive effect via acting as a skin protective barrier. Furthermore, chamomile oil has crucial effect in promoting the re-epithelization rate and stimulating the collagen deposition [10]. However, the poor membrane permeability and degradation of the chamomile oil after exposure to oxygen, humidity and light account for the limitations of its direct application as a topical wound treatment. Encapsulation of CM oil into lipid nanocarriers can protect it and enhance its therapeutic effect in wound healing [11].

Lipid nanoparticles have emerged as an optimum topical carrier owing to their high biocompatibility, ability to encapsulate a wide range of both natural and semi-synthetic drugs, high drug load and large-scale production. In addition, they are suitable carriers to be applied to damaged and inflamed skin and they have a well reported occlusive property based on their lipid nature, which is an important factor in accelerating wound healing [12].

Many studies have investigated the efficient use of lipid nanocarriers for the successful intracellular delivery and the protection of phytochemical and therapeutic molecules [13–15]. Gainza et al. demonstrated the potential use of recombinant human epidermal growth factor (rhEGF) loaded lipid nanoparticles for the management of chronic wounds [16]. Results suggested that the encapsulation of rhEGF into solid lipid nanoparticles (SLN) and nanostructured lipid carries (NLC) improve its stability and allowed its sustained delivery. Further studies included the encapsulation of human antimicrobial peptide in NLC for chronic wound healing [17] and the use of curcumin loaded nanostructured lipid dispersion as anti-proliferative agent for the treatment of psoriasis [18].

The present study aimed to overcome the drawbacks of the direct application of CM. The study investigated the ability of SLN to encapsulate and improve CM therapeutic effect including its penetration through skin layers with subsequent enhancement in its anti-inflammatory and healing properties. The formulations were evaluated histologically, histochemically and biochemically in wounded rats.

2. Materials and methods

2.1. Materials

Stearic acid (SA), formalin and paraplast N were purchased from Fischer scientific, UK. Polysorbate 80 (Tween 80), hematoxylin, fast green FCF (CI: 42053) and mercuric oxide were purchased from Merck, Germany. Chamomile oil (CM) was purchased from local herbal market (Harraz Co.), Egypt. Xylene, glacial acetic acid, potassium alum, absolute ethyl alcohol, N-butyl alcohol and ferric ammonium sulfate were purchased from El-Nasr Pharmaceutical Co., Egypt. Camisan® cream (contains ethanol extract of Chamomile 2 mg, and essential oil 20 mg EIPICO, Egypt). Ketamine HCL and xylazine solutions were provided from Abbott Laboratories. Terpineol anhydrous was purchased from Fluka AG, Buchs SG, Switzerland. DPX mountant was purchased from Park Scientific limited, Northampton, UK. Acid fuchsin (CI: 42685) and ponceau de xylidine (CI: 16150) were purchased BDH Chemicals Ltd., Poole, England. Phosphomolybdic acid was purchased from Prolabo, Paris, France. Picric acid 99.5% A.R. was purchased from Oxford Laboratory, Mumbai, India. Eosin Y (CI: 45380) was purchased from Riedel-de Haën Chemicals, Seelze, Germany.

2.2. Methods

2.2.1. Preparation of solid lipid nanoparticles

Solid lipid nanoparticles (SLN) were prepared using hot homogenization method [19]. Briefly, lipid phase formed of 20% w/w of SA with different ratios of CM were heated to 60 °C. An aqueous phase containing 5%w/w Tween 80 heated to the same temperature was added to the lipid phase and homogenized at 24, 000 rpm for 3 min using high shear homogenizer (Ultra Turrax T25; IKA, Staufen, Germany). Cooling of the nanoemulsion allowed the formation of SLN. Table 1 shows the composition of the prepared formulations.

2.2.2. Characterization of solid lipid nanoparticles

2.2.2.1. Particles morphology, particle size distribution and zeta potential. SLN morphology was examined using transmission electron microscope (JEM-1010, JEOL Ltd, Tokyo, Japan). Selected formula of SLN was diluted and 1 µl of the dispersion was placed on a carbon-coated grid. The suspension was left for 2 min to allow its absorption in the carbon film, and then microscopically examined at high resolution (20,000 kV).

The particles size, polydispersity index (PDI) and the zeta potential of the diluted SLN were determined by dynamic light scattering particle size analyzer (DLS, Zetasizer Nano ZS, Malvern instruments, Worcestershire, UK) at 25 °C [19].

2.2.2.2. Occlusion test and viscosity measurements. The ability of the formed SLN to form an occlusive film was investigated using the procedure adapted by Gainza et al. [20]. Briefly, a fixed volume of SLN was spread on the surface of filter membrane (dialysis cellulose membrane, Sigma- Aldrich) to form a film and placed on Franz cell containing 5 ml of water. Cells without sample served as a reference. The samples were kept at 32 °C for 48 h and weighted at the beginning and at the end of the experiment to obtain the water loss due to evaporation. The occlusion factor (F) was calculated using the following equation:

$$F = ((A-B)/A) * 100$$

Where A is the water loss without sample (reference) and B is the water loss with sample. An occlusion factor of 0 means no occlusive effect compared to the reference and 100 is the maximum occlusion factor.

The rheological properties of the SLN dispersions were estimated by measuring the viscosity of 1 ml of the dispersion at a shear rate of $10\,s^{-1}$ at 25 ± 0.1 °C °C using cone and plate programmable viscometer (Brookfield Engineering Laboratories Inc., Model HADV-II,

USA) connected to a digital thermostatically controlled circulating water bath (Polyscience, Model 9101, USA) with spindle 52. The sample was left to equilibrate for 2 min after viscometer loading [21]. All obtained results were the average of three readings.

2.2.2.3. Differential scanning calorimetry. The effect of different ratios of CM on the thermal behavior of SLN was investigated using differential scanning calorimeter (Shimadzu-DSC 60, Kyoto, Japan). Lyophilized samples (2–3 mg) were placed in aluminum pans with lids and heated to a temperature of 220 °C at a rate of 10 °C/min, using dry nitrogen as a carrier gas with a flow rate of 25 ml/min.

2.3. In-vivo biological study

2.3.1. Animals

A total of 40 adult male Wistar rats weighing 150–175 g obtained from the breeding unit of the Medical Research Center (Faculty of Medicine, Ain Shams University, Cairo) were used throughout this study. The rats were housed in well-aerated standard stainless-steel cages and maintained under laboratory conditions (temperature 22 ± 2 °C, and 12 h-12 h light/dark cycle) with proper human care. They were given free access to food and water and acclimatized for a week before the start of the experiment. Experimental protocol was approved by the local institutional animal ethics committee of Ain Shams University.

2.3.2. Experimental design

The rats were randomly divided into 5 groups of 8 rats each. Group I: Animals served as normal control; without wounding. Group II: Animals were wounded and kept without treatment for 16 days, serving as untreated control group. Groups III to V: Animals were wounded and topically treated daily for 16 consecutive days with different formulae. Group III was topically treated with plain solid lipid nanoparticles (SLN-F1), group IV was topically treated with chamomile oil cream (CM) and group V was topically treated with chamomile-loaded solid lipid nanoparticles (CM-SLN-F3). On day 16, the animals were sacrificed through diethyl ether inhalation.

2.3.3. Formation of the excision wound

All rats from group II to V were anesthetized with an intraperitoneal injection of Ketamine HCL solution (90 mg/kg b.w.) and xylazine (10 mg/kg b.w.) [22]. Their backs were shaved, and round full-thickness excisional wounds of 2 cm diameter were generated by using sterile steel scalpel.

2.3.4. Evaluation and assessment of wound healing

In order to assess the effectiveness of the topical use of different formulations on the wound area closure, created wounds were photographed using a digital camera on day 1, 8 and 16 of the experiment. The wound area was measured using tracing transparent paper, and the percentage of wound healing was calculated by Walker and Masson [23] formula after measuring the wound area as follows:

$$\text{Percentage of wound area} = \frac{\text{wound area in day X}}{\text{wound area in the first day}} \text{X } 100$$

Percentage of wound healing = 100 - percentage of wound area

2.3.5. Histological and histochemical evaluation

For the histological evaluation, three rats were randomly selected from each experimental group on 16th day after wound creation, and then the skin samples representing the wound area and surrounding tissue were excised and fixed in aqueous Bouin's fluid for 24 h. The fixed tissues were then embedded in paraplast and serial sections were made at a thickness of 5–6 μm and stained with Harris hematoxylin and eosin [24]. Moreover, selected sections were stained with Masson trichrome stain to evaluate the dermal collagen [25].

The re-epithelization process was measured according to the criteria established by Sinha and Gallagher [26]: 1, re-epithelization at the edge of the wound; 2, re-epithelization covering less than half of the wound; 3, re-epithelization covering more than half of the wound; 4, re-epithelization covering the entire wound with irregular thickness; and 5, re-epithelization covering the entire wound with regular thickness.

2.3.6. Biochemical investigations

The skin samples allocated from each group, including wound area were harvested on day 16, kept in saline solution (0.9%) and stored at −20 °C for the biochemical investigation.

2.3.6.1. IL-1β and TGF-β1 assessment. IL-1, one of the potent pro-inflammatory cytokine was quantitatively determined in the wound tissue homogenates from all groups using the rat interleukin-1β ELISA kit (CUSABIO kit; USA; Cat. No. CSB-E08055r). At the same time, TGF-β1 being one of the main member of the TGF-β family which is involved in all stages of wound healing process, was assessed using the rat transforming growth factor β1 (TGF-β1) ELISA kits (CUSABIO, USA; Cat.No. CSB-E04727r) according to the instructor's protocol.

2.3.6.2. Collagen deposition determination. Collagen-1 accumulation was quantitatively determined in the wound tissue homogenates from all groups using the rat collagen alpha-1(I) chain (COL1A1) ELISA kit (My Bio Source.co. San Diego, USA; Cat.No. MBS701594) according to the instructor's protocol.

2.3.6.3. Assessment of metalloproteinases (MMP-9) and their tissue inhibitors (TIMP-1) activities. In order to evaluate the tissue remolding phase for the different formulations used in the present study, MMP-9 (gelatinase B) was analyzed using the rat matrix metalloproteinase 9/gelatinase B (MMP-9) ELISA kit (CUSABIO, USA; Cat. No. CSB-E08008r). Also, TIMP-1 level was analyzed using the ELISA kit, purchased from Kamiya Biomedical Company (USA; Cat. No. KT-30034) according to the manufacture's procedure.

2.4. Statistical analysis

The *in-vitro* data obtained were compared using one-way analysis of variance, followed by multiple comparisons of Tukey–Kramer test using Graph Pad6 Instat® software (GraphPad Software, La Jolla, CA). The significance level was at $p \leq 0.05$. For *in-vivo* study, statistical analysis was performed using the Statistical Package for the Social Science (SPSS) for Windows (version 22.0, Chicago, IL, USA). Results were expressed as mean values ± SD. Data were analyzed by *t*-test and one-way analysis of variance (ANOVA). Statistical probability; $p < 0.05$ was assigned as statistically significant.

3. Results

3.1. Physicochemical characterization of chamomile oil loaded solid lipid nanoparticles

SLN were successfully prepared using 20% w/w of the SA as lipid matrix which is the generally used lipid concentration to get the semisolid appearance. TEM image of the formed particles (Fig. 1) shows the structure of the selected SLN (SA: CM oil in ratio 7:3). As revealed, CM oil forms an outer shell surrounding the lipid core. The particle size, PDI and zeta potential of the prepared SLN are shown in Table 1. SLN prepared at 9:1 and 7:3 of SA: CM showed a lower particle size than those prepared without CM oil (plain SLN, F1). In contrast, SLN prepared at a ratio of 1:1 of SA: CM oil (F4) showed a significantly ($p < 0.05$) larger size than other SLN, even it approached microparticles. The prepared SLN showed a homogenous particle size

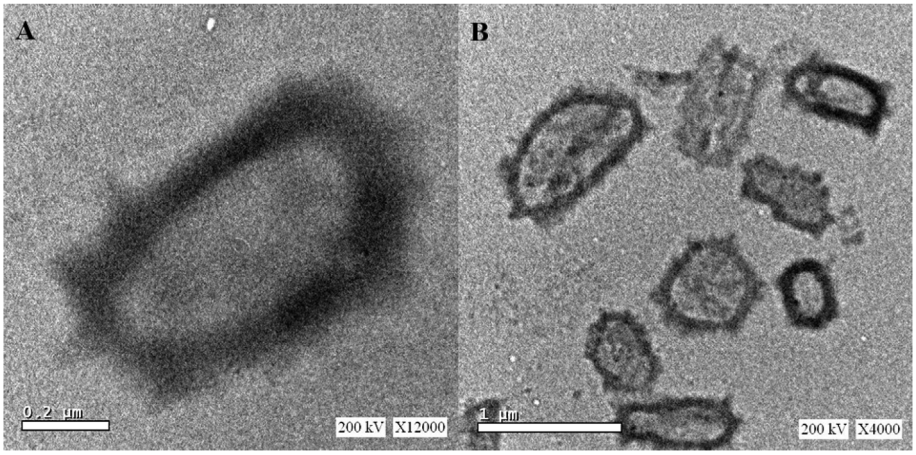

Fig. 1. Transmission electron microscope of chamomile oil solid lipid nanoparticles.

distribution with PDI values less than 0.4 except that prepared at 1:1 of SA: CM. All the prepared SLN revealed zeta potential values ranging from −25.6 to −35.9 mV.

3.2. Occlusion factor and viscosity measurement

The viscosity and the occlusion factor of the formed SLN dispersions are shown in Table 1. A significant difference ($p < 0.05$) in occlusion factor was determined upon varying CM oil ratio in the formed SLN. The highest occlusion factor was observed with SLN prepared without CM oil (F1) followed by those prepared with 9:1 and 7:3 of SA: CM and finally, SLN prepared with equal ratio of SA and CM. In addition, SLN showed a significant ($p < 0.05$) decrease in viscosity with increasing the CM ratio.

3.3. DSC study

The DSC profiles of SA, SA + CM mixture, in addition to the different prepared SLN are shown in Fig. 2, while Table 2 shows their corresponding melting peaks and enthalpies. As observed, SA showed a sharp endothermic peak at 57.05 °C with a slight shift to 56.74 °C upon mixing with CM oil. The obtained DSC thermograms revealed the significant effect of CM oil presence on the melting properties of the formed SLN. Increasing CM oil ratio in the lipid matrix of the prepared SLN (starting from F1 to F4) resulted in decreasing the melting points and the melting enthalpies of the formed lipid matrix with an obvious shift in the endothermic peaks.

Table 2
Melting Peaks and Enthalpies of chamomile oil–loaded SLN.

Formulation	Onset (°C)	Melting peak (°C)	End (°C)	Enthalpy (J/g)
SA	54.88	57.05	60.47	−513.83
SA + CM	52.16	56.74	60.26	−486.21
F1	51.95	55.32	57.73	−223.84
F2	49.18	53.51	56.06	−206.65
F3	45.77	51.52	54.25	−160.39
F4	39.08	48.15	53.76	−97.23

3.4. In-vivo study

3.4.1. Wound closure and healing assay

The impact of the topical application of the formulations (plain SLN, CM-SLN, CM cream) on the wound closure was morphologically

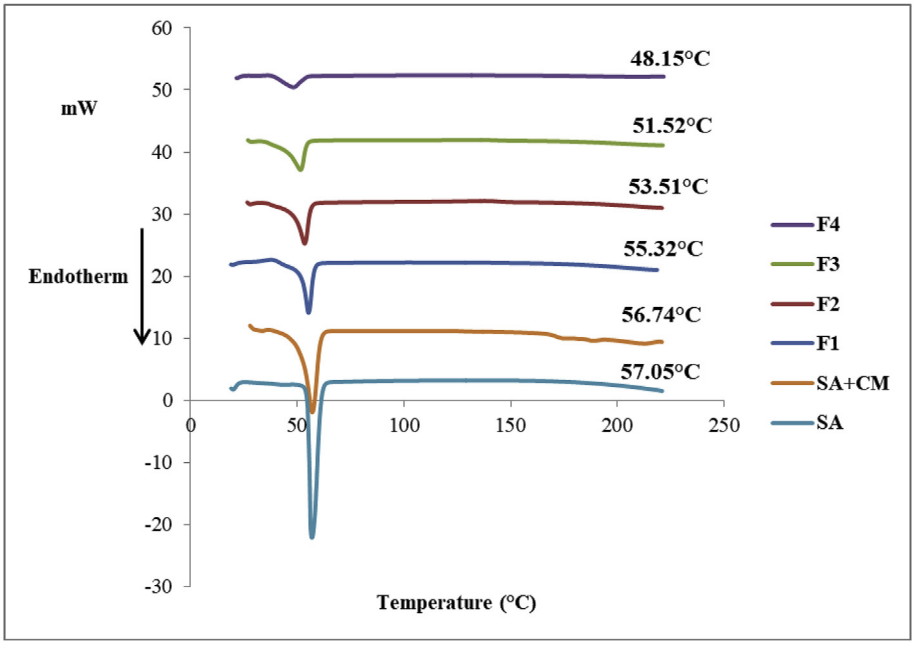

Fig. 2. Differential scanning calorimetry thermograms of different solid lipid nanoparticles showing effect of chamomile oil ratio on melting point. (F1, F2, F3 and F4: solid lipid nanoparticles with stearic acid to chamomile oil in ratios of 10:0, 9:1, 7:3 and 1:1 respectively; SA + CM: stearic acid and chamomile oil physical mixture; SA: stearic acid.

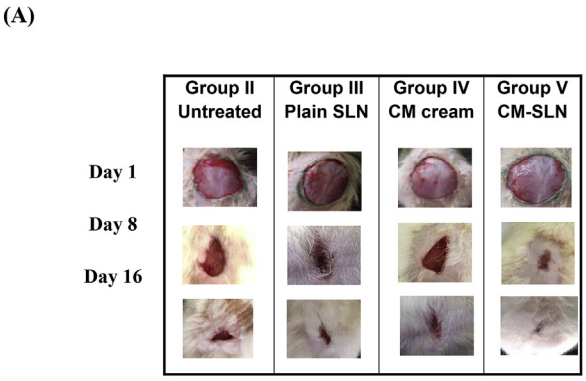

Fig. 3. Effect of solid lipid nanoparticles (plain SLN), chamomile oil cream (CM cream) and chamomile-loaded solid lipid nanoparticles (CM-SLN) formulations on the wound closure and healing activity *in vivo*. (a): illustrative images for the different groups of rats topically treated with the different formulations on day 1, 8 and 16 post wounding. (b): representative graphs for the percentage reduction in the wound area that reflecting the increase in the healing activity percentage. Results are expressed as mean ± SEM of the 8 rats from each group. $^{*a}p < 0.05$ compared to untreated wounded animals, $^{\#a}p < 0.001$ compared to untreated group, $^{\#b}p < 0.001$ compared to SLN group and $^{\#c}p < 0.001$ compared to CM group.

evaluated by calculating the wound area on day 1, 8 and 16 after injury. As shown in Fig. 3 (A & B), plain SLN and CM cream exhibited significant reduction in the wound area on day 8 and 16, compared to the untreated animals. Fortunately, the CM-loaded SLN was shown to accelerate the healing activity percentage, reaching 96% on day 16. Moreover, this formulation evoked the lowest significant ($p < 0.001$) percentage of wound area, regarding to their respective control groups; untreated, plain SLN and CM cream.

3.4.2. Histological and histochemical investigation

The microscopical investigation of the rat skin of the control group (GI) reveals that it consists of two layers, namely: the epidermis and dermis (Fig. 4A). The former layer is thin (mean thickness of about 29 μm) and is built up of a stratified squamous keratinizing epithelium which is divided into four layers of keratinocytes, namely: the *stratum germinativum*, *stratum spinosum*, *stratum granulosum* and *stratum corneum*. The *stratum germinativum* is formed of single layer of cuboidal cells, while the *stratum spinosum* is built up of large polyhedral cells. In addition, the cells of *stratum granulosum* are flattened and spindle in shape and their cytoplasm appeared to contain abundant basophilic granules. The *stratum corneum*, the superficial non-cellular layer, consists of many layers of flattened non-nucleated acidophilic keratinized cells (Fig. 4B). Moreover, the dermal layer is formed of dense fibro-elastic connective tissue that contains numerous hair follicles, sebaceous and sweat glands (Fig. 4C).

The evaluation of the re-epithelization grade according to the criteria of Sinha and Gallagher (2003) [26] revealed that the untreated and the plain SLN treated groups showed incomplete re-epithelialization of grade 3, while the CM cream and CM-SLN treated groups showed irregular complete re-epithelialization of grade 4 (Fig. 5A–D). Moreover, there was subcorneal and intraepidermal pustules filled with neutrophils and lymphocytes in the untreated group (Fig. 5A), while the open wound area was covered by fibrin clot and inflammatory cells in the plain SLN group (Fig. 5B).

The histological investigation of the skin of rats of the untreated group (GII) revealed many histopathological effects in the regenerated epidermis that included a flat acanthosis (epidermal hyperplasia) with mean thickness of about 119 μm. In addition, there was parakeratosis that was caused by incomplete keratinization in which nuclei remained in the cells of the *stratum corneum*. Moreover, there was a spongiosis (intercellular edema between neighboring keratinocytes) and intracellular edema or ballooning degeneration (infiltration of cytoplasm into keratinocytes, as the swelling develops; the cells deform and become spherical). Some keratinocytes had pyknotic nuclei (Fig. 6A).

Wounds of the group III, topically treated with the plain SLN, were open and their edges had disorganized epidermal cell layers (Fig. 6B) and the re-epithelialized epidermis showed a flat acanthosis with mean thickness of about 82 μm (Fig. 6C). Moreover, there was spongiosis, intracellular edema and some keratinocytes had pyknotic nuclei (Fig. 6B and C). Moreover, few keratinocytes had been keratinized abnormally before they reached the horny cell layer (dyskeratosis) (Fig. 6C).

The re-epithelialized epidermis of the group IV topically treated with CM cream was covered by a hard protective crust on the surface known as a scab. The formation of a scab is a part of the healing process as skin grows over the wound (Figs. 5C and 6D). The skin of this group showed some histopathological alterations that included a flat acanthosis with mean thickness of about 86 μm (Fig. 6E). Moreover, a spongiosis, intracellular edema and keratinocytes with pyknotic nuclei were noticed (Fig. 6D and E).

Wounds of the group V topically treated with CM-SLN showed a flat acanthosis with mean thickness of about 85 μm (Fig. 5D). The epidermal layer was organized and showed normal histological structure nearly without remarkable alterations as compared to the control group (Fig. 6F).

The dermal layer of the untreated and all treated groups had granulation (repair) tissue with many inflammatory cells (lymphocytes), numerous fibroblasts and collagen fibrils. It is noteworthy to

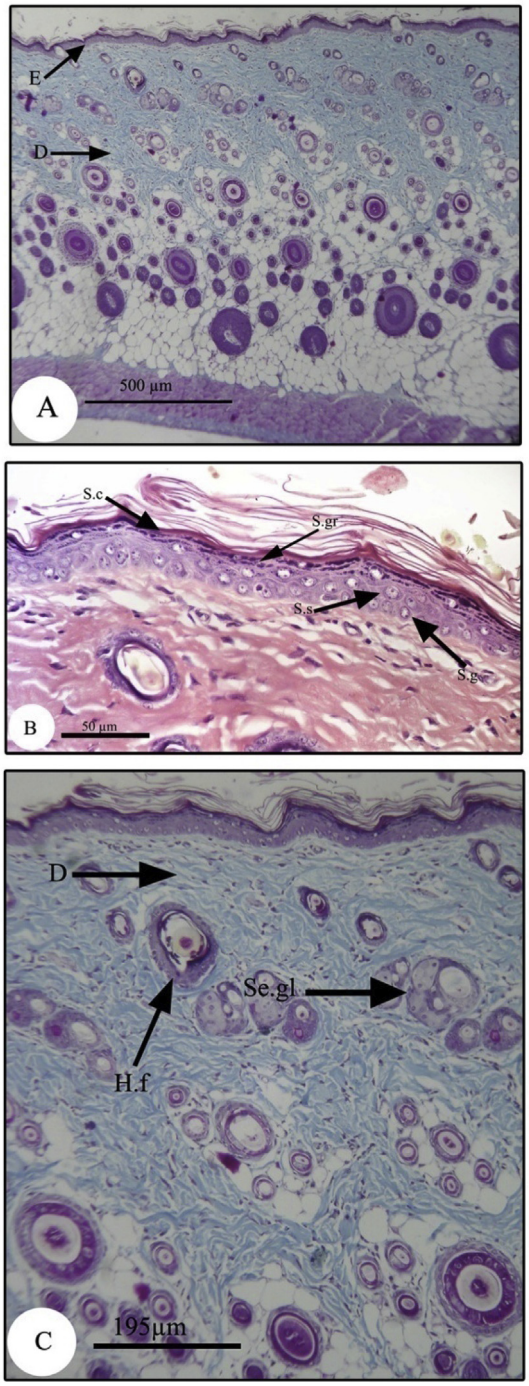

Fig. 4. (A–C): V.S. of skin of rat of control group, showing the normal skin structure. D: dermis, E: epidermis, H.f: hair follicle, S.c: stratum corneum, S.g: stratum germinativum, S.gr: stratum granulosum, S.s: stratum spinosum and Se.gl: sebaceous gland. A & C were stained by Masson's trichrome, and B was stained by Hx & E.

mention that the CM-SLN group had more collagen fibrils deposition than that of the untreated, plain SLN and CM groups (Fig. 7A–D).

3.4.3. Biochemical investigations

The results of all the biochemical parameters investigated in the present study are summarized in Table 3.

3.4.3.1. Effect of tested formulations on the interleukin-1 beta (IL-1β) level. As shown in Table 3, the untreated wounded animals exhibited significant increase ($p < 0.001$) in the IL-1β, compared to the normal control. This reflects the inflammatory state of the wounded tissue. As revealed, the topical application of the plain SLN and CM cream formulations were shown to ameliorate this inflammatory stage via reducing the IL-1β level. Furthermore, the topical use of CM-SLN formulation on the wounded animals was shown to rebound this pro-inflammatory cytokine (IL-1β) almost to the normal control level, with the highest significant ($p < 0.001$) reduction in its level, compared to the untreated wounded animals.

3.4.3.2. Transforming growth factor-beta (TGF-β1) level in wound-tissues. The present results revealed dramatic and significant decrease ($p < 0.001$) in the TGF-β1 level in the untreated wounded animals (group II), compared to the normal control group, indicating the slower healing rate. On the other hand, wounds treated with plain SLN formulation (group III) showed marginal and significant ($p < 0.001$) restore in the TGF-β1 level, compared to the untreated group. While, topical application of CM cream (group IV) exhibited significant increase ($p < 0.001$) in the TGF-β1 level. Moreover, the CM-SLN (group V) showed the highest significant increase in the TGF-β1 level, compared to the untreated, plain SLN and CM cream. These results are consistent with the morphological evaluation reflecting the wound closure.

3.4.3.3. Collagen-1 content in wound area treated with different formulations. The current results revealed highest significant amount of collagen deposited in the wound of animals treated with the CM-SLN formulation, which was directly correlated with the wound contraction, compared with the untreated, plain SLN and CM cream groups (Table 3).

3.4.3.4. Metalloproteinases (MMP-9) activities and their inhibitors (TIMP-1) in healing process. As shown in Table 3, the untreated wounded animals exhibited significant ($p < 0.001$) increase in the MMP-9 activity, compared to the normal control group. Additionally, the highest MMP-9/TIMP-1 calculated ratio was observed in this untreated group. These findings indicated the poor healing rate compared to the other treated groups. On the other hand, the topical application of the CM-SLN formulation exhibited the lowest significant ($p < 0.001$) MMP-9 activity in the wounded animal tissues collected on 16th post injury day, compared to the untreated group, plain SLN and CM cream formulations. Furthermore, it was accompanied by the highest activities in their relative inhibitors (TIMP-1).

4. Discussion

Lipid nanoparticles have been investigated as an interesting drug delivery system for the treatment of wounds in previous studies. Favorable properties of SLN for wound treatment include small size, lipid composition, high contact between drug and skin, in addition to occlusive properties which increase skin hydration [16,20]. Stearic acid being a naturally occurring lipid has many therapeutic benefits including anti-bacterial and anti-inflammatory effect [27], therefore it was chosen as the lipid matrix to prepare SLN.

The drug-enriched shell model of the obtained CM loaded SLN shown in Fig. 1A is attributed to the used method of preparation. During hot homogenization, all lipid components are in liquid state. However during cooling of the lipid matrix, SA owing to its higher melting point than CM oil showed a more rapid solidification rate forming the solid lipid core with part of CM oil distributed in the matrix and the excess amount located at the outer shell [28,29]. The irregular shape of the formed SLN is attributed to the presence of relatively high amount CM oil (7:3 of SA: CM) in the lipid matrix. Liquid lipid can form oil nanocompartments within the lipid matrix as demonstrated by the appearance of dark spots on the core of the particles (Fig. 1B), while excess liquid lipid adhere to the particles surface causing irregular

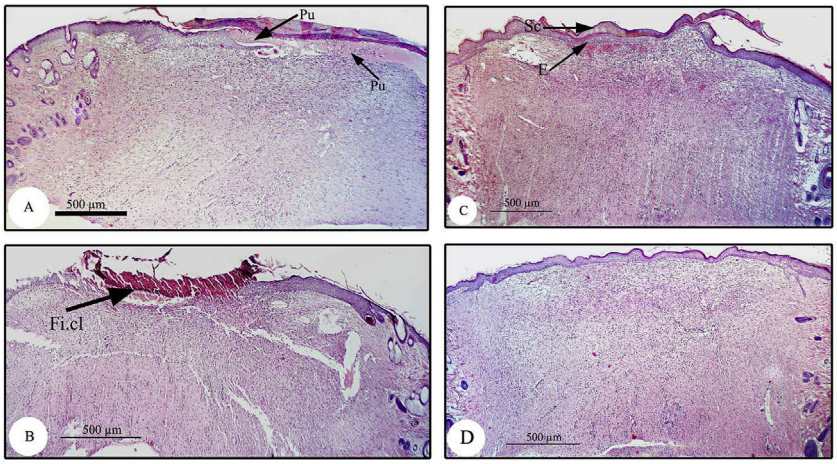

Fig. 5. (A–D): V.S. of skin of rat A: untreated group, B: plain SLN group, C: CM cream group and D: CM-SLN group, showing the re-epithelization grade. E: epidermis, Fi.cl: fibrin clot, Pu: pustule and Sc: scab. Hx & E stain.

shape due to its greater mobility [29,30].

Presence of chamomile oil in the lipid matrix resulted in decreasing the particle size of the formed SLN (from 619 nm in F1 without chamomile oil to 572.8 nm in F2 with 9:1 of SA: CM and 524.1 nm in F3 with 7:3 of SA: CM), which may be attributed to the decreased viscosity of the lipid matrix due to the addition of CM oil and, hence, decreasing the surface tension. However, further increase in chamomile ratio (F4 with ratio 1:1 of SA: CM) caused a distortion of the matrix core of the nanoparticles, with subsequent larger particle size (956.5 nm) than other SLN, which even approached microparticles. PDI and zeta potential values indicate the homogenous distribution and the high stability of the prepared particles respectively, in which the negative charge is attributed to lipid matrix of SA.

Occlusion factor give an indication about the ability of the formulation to keep the wound hydrated. Wound hydration is an essential factor to be considered in accelerating wound healing process. Lipid

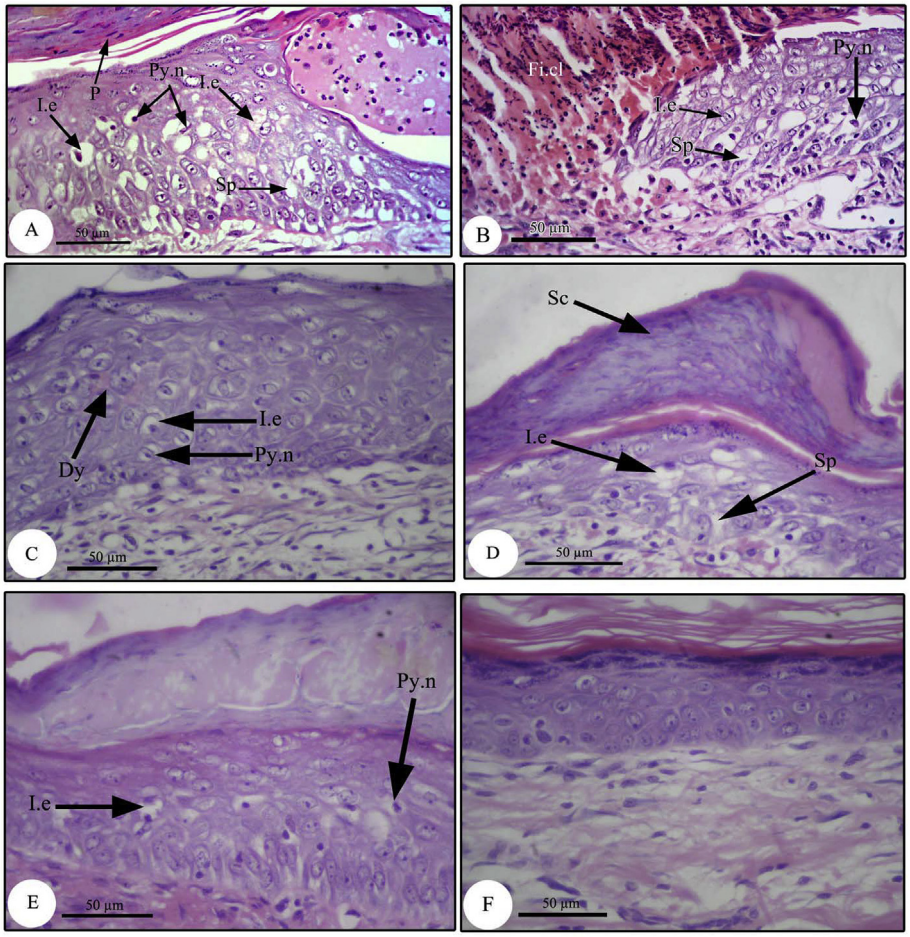

Fig. 6. (A–F): V.S. of skin of rat A: untreated group, B-C: plain SLN group, D–E: CM cream group and F: CM-SLN group, showing the histopathological features of the epidermis. Dy: dyskeratosis, Fi.cl: fibrin clot, I.e: intracellular edema, P: parakeratosis, Py.n: pyknotic nuclei, Sc: scab and Sp: spongiosis. Hx & E stain.

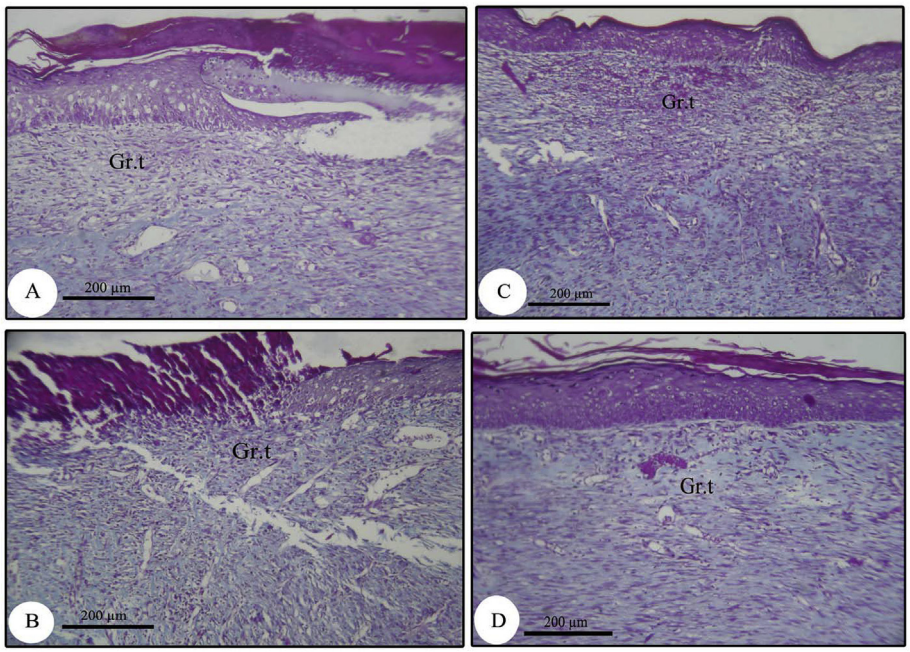

Fig. 7. (A–D): V.S. of skin of rat A: untreated group, B: plain SLN group, C: CM cream group and D: CM-SLN group, showing the granulation tissue (Gr.t). Masson's trichrome stain.

nanoparticles have the ability to form an occlusive film, minimizing water loss from the skin with enhanced skin hydration. However, occlusive effect varies depending on melting point of the lipid, size of the formed nanoparticles and liquid lipid content. It has been reported that highest occlusion effect of lipid nanoparticles can be obtained using particles with small size and low melting point lipids [31,32]. SA is characterized by low melting of which can contribute to higher occlusion in comparison to other lipids [27].

The highest occlusion factor was observed with SLN prepared without CM, which is attributed to the effect of the more solidified matrix obtained in comparison to the more liquefied matrix containing chamomile oil. It has been reported that the more solid matrix prevents more water evaporation with higher occlusion effect [16,33]. SLN showed a significant ($p < 0.05$) decrease in viscosity with increasing the CM ratio. The presence of CM oil allowed the production of SLN with high lipid content and at the same time with acceptable viscosity to be applied to the wound topically.

In addition DSC thermograms revealed the effect of CM oil presence on the thermal properties of the formed SLN. All prepared SLN showed a decrease in both the melting point of SA and in the enthalpy revealing the effect of SLN formation on decreasing the lipid crystallinity. Moreover, the broadening of the obtained peaks indicates the formation of less ordered crystal lattice delaying the recrystallization of the lipid matrix during the cooling process due to presence of CM oil [34,35].

In order to investigate the effect of the lipid nanoparticles on wound healing, plain SLN without CM oil, in addition to Camisan® cream were included in the *in-vivo* study. F3 containing SA to CM in ratio 7:3 was chosen in the in-vivo study due to its acceptable particle size, PDI, zeta potential and occlusive properties.

In the present study, the epidermal layer of the CM cream treated group showed histological improvement in comparable with that of the untreated and plain SLN groups, moreover, the epidermal layer of the CM-SLN treated group showed more or less normal histological structure nearly without remarkable histological alterations. The obtained results may be due to the effect of chamomile oil on promoting faster re-epithelization and tissue granulation [36,37].

Moreover, the epidermal layer of the CM-SLN group showed better histological improvement in comparable with that of CM cream group. Accordingly, the improved wound healing promoted by the encapsulated CM compared with the free CM confirms that SLN encapsulation improves the stability of CM due to protection from the wound environment and oxidative stress [38]. Moreover, SLN allows a controlled release profile of CM which may provide a sustained concentration of CM in the wound area, and stimulates fibroblast and

Table 3
Collective table of the effect of different formulations used for wound healing on the studied biochemical parameters.

Mean ± SD	Groups				
	Group I Normal control	Group II Untreated	Group III Plain SLN	Group IV CM cream	Group V CM-SLN
IL-1β (pg/mg)	130.4 ± 0.52	168.3 ± 0.58$^{\#a}$	157.17 ± 0.76$^{\#b}$	155.5 ± 0.5$^{\#b}$	145.8 ± 0.76$^{\#bcd}$
TGF-B1 (pg/mg)	16.04 ± 0.08	12.0 ± 0.1$^{\#a}$	12.7 ± 0.1^{*b}	13.13 ± 0.08$^{\#b}$	14.1 ± 0.2 $^{\#bc*d}$
Col-1 (ng/mg)	5.46 ± 0.04	3.03 ± 0.1$^{\#a}$	3.57 ± 0.1^{*b}	3.8 ± 0.2$^{\#b}$	4.6 ± 0.06$^{\#bcd}$
MMP-9 (pg/mg)	21.89 ± 0.09	30.93 ± 0.9$^{\#a}$	28.80 ± 0.2$^{\dagger b}$	28.2 ± 0.23$^{\dagger b}$	26.3 ± 0.32$^{*b\#c*d}$
TIMP-1 (ng/mg)	5.5 ± 0.2	2.7 ± 0.1$^{\#a}$	3.03 ± 0.06$^{\dagger b}$	3.27 ± 0.25$^{\dagger b}$	4.67 ± 0.29$^{\#bc\dagger d}$
MMP-9/TIMP-1	3.98	11.45$^{\#a}$	9.50 $^{\#b}$	8.62$^{\dagger b}$	5.63$^{\#bc*d}$

IL-1β, interleukin-1β; TGF-β1, transforming growth factor-β; Col-1, collagen-1; MMP-9, metalloproteinase-9; TIMP-1, tissue inhibitor metalloproteinase-1. Results are expressed as mean ± SD. $^{\#a}$P value < 0.001 when compared to the normal control group, $^{\#b}$P value < 0.001 when compared to the untreated group, $^{\#c}$P value < 0.001 when compared to the SLN group, $^{\#d}$P value < 0.001 when compared to the CM group, ^{*b}P value = 0.001 when compared to the untreated group, ^{*d}P value = 0.001 when compared to the CM group and $^{\dagger b}$P value < 0.05 when compared to the untreated group.

keratinocyte proliferation and differentiation [39]. In addition, it should be noted that SLN are a very well-tolerated delivery system with occlusive properties that can increase skin hydration [40].].

The presence of subcorneal and intraepidermal pustules filled with neutrophils and lymphocytes in the untreated group and the presence of numerous inflammatory cells in the wound area of the plain SLN group indicate that permanent neutrophil infiltration may be involved in wound healing delay, as neutrophils release an excessive amount of proteases that degrade the extracellular matrix [41].

Moreover, the CM-SLN group showed better improvement in wound healing, as it enhanced collagen deposition in the dermal layer compared to the untreated, plain SLN and CM cream groups that have a mild collagen deposition. Chamomile contains high amounts of proline and leucine amino acids which are involved in the collagen synthesis [37].

In the present study, the highest reduction in the IL-1β level was detected in the group of animals treated with the CM-SLN formulation as compared to the untreated, plain SLN and CM cream groups reflecting the crucial effect of SLN in improving the anti-inflammatory activity of CM, as well as limiting tissue damage caused by inflammation and hence accelerating its healing activity. These observations are in accordance with Krausz et al. [41], who stated that the IL-1β reduction was essential in attenuating the inflammatory response and accelerating the healing activity. The anti-inflammatory activity of chamomile was due to its active constituents such as flavonoids, α-bisabolol and spiroether. Furthermore, many polyphenolic compounds and volatile oils in chamomile are capable to reduce the expression of different pro-inflammatory cytokines, including IL-1β [42].

During the proliferative phase, the highest level of TGF-β1 was detected in the group of animals that were topically treated with CM-SLN formulation. Based on the vital and crucial role of TGF-β1 in improving the angiogenic properties of the endothelial cells and stimulating the fibroblast contraction [2], these findings indicated that the loading of chamomile oil on the SLN improved its healing activity via restoring the TGF-β1 level and hence accelerating the re-epithelialization, proliferation and tissue remolding [3].

The correlation between the TGF-β1and collagen production was clarified throughout this study, since the highest ability of CM-SLN formulation to restore the TGF-β1 was accompanied with the maximum amount of collagen accumulated within the wound sites, compared to the untreated, plain SLN and CM cream groups. On the other hand, slower wound repair was characterized by impaired recruitment of fibroblasts, and therefore, reduced collagen deposition, as observed in the untreated group. The chamomile impact on promoting the healing activity via collagen synthesis was due to its main bioactive constituents [43].

Results from this study indicated that the slowest healing rate was reported in the untreated wounded animals compared with the other treated groups, as showed by the significantly high MMP-9 activity ($p < 0.001$), in addition to the lowest activity in its relative inhibitor, TIMP-1. On the other hand, treatment with CM-SLN formulation has brought back the MMP-9 activity near to that in the normal tissue besides restoring the TIMP-1 level, indicating the highest healing rate activity of this formulation, compared to the plain SLN and CM cream ones. MMP-9 is mainly expressed by neutrophils and macrophages, which are essentially involved in the inflammatory response [44]. In addition, Sabino & Keller [4] postulated that the ability of IL-1β to synthesizes MMPs and suppresses TIMPs at the same time clarifies the directly proportional relationship between the IL-1β level and MMP-9 activity observed in the present study. Accordingly, the high levels of MMP-9 and IL-1β were actually linked with slow healing rate, as shown in the untreated group. Conversely, the low levels of MMP-9 and IL-1β were concomitant with the fastest healing rate, as detected in the CM-SLN formulation, compared to the plain SLN and CM cream groups.

It is noteworthy to note that the highest MMP-9/TIMP-1 ratio was observed in the untreated group indicating the slowest healing rate. While, the lowest MMP-9/TIMP-1 ratio, observed in the treated group with CM-SLN formulation was accompanied by the fastest wound contraction and hence the best healing rate activity, compared to either plain SLN or CM cream formulations [45].

5. Conclusions

The results of the present study revealed the essential role of solid lipid nanoparticles in improving the penetration of chamomile oil through biological barrier and hence accelerating the wound healing activity rate. This was confirmed by their enhancing effect on the wound area contraction, increased the re-epithelization grade, increased collagen deposition, skin architecture, increased tensile strength, increased the TGF-β levels and decreased in the IL-1β levels and MMP-9 activity.

Appendix A. Supplementary data

Supplementary data to this article can be found online at https://doi.org/10.1016/j.jddst.2019.01.008.

References

[1] K. Järbrink, G. Ni, H. Sönnergren, A. Schmidtchen, C. Pang, R. Bajpai, et al., Prevalence and incidence of chronic wounds and related complications: a protocol for a systematic review, Syst. Rev. 5 (1) (2016) 152–157.
[2] M. Pakyari, A. Farrokhi, M.K. Maharlooei, A. Ghahary, Critical role of transforming growth factor beta in different phases of wound healing, Adv. Wound Care 2 (5) (2013) 215–224.
[3] A. Vasconcelos, A. Cavaco-Paulo, Wound dressings for a proteolytic-rich environment, Appl. Microbiol. Biotechnol. 90 (2) (2011) 445–460.
[4] F. Sabino, U.A.D. Keller, Matrix metalloproteinases in impaired wound healing, Metalloproteinases Med. 2 (2015) 1–8.
[5] A.D. Widgerow, Nanocrystalline silver, gelatinases and the clinical implications, Burns 36 (7) (2010) 965–974.
[6] R.E. Mirza, M.M. Fang, W.J. Ennis, T.J. Koh, Blocking interleukin-1β induces a healing-associated wound macrophage phenotype and improves healing in type 2 diabetes, Diabetes 62 (7) (2013) 2579–2587.
[7] M.C. Robson, D.A. Dubay, X. Wang, M.G. Franz, Effect of cytokine growth factors on the prevention of acute wound failure, Wound Repair Regen. 12 (2004) 38–43.
[8] D. Dwivedi, M. Dwivedi, S. Malviya, V. Singh, Evaluation of wound healing, antimicrobial and antioxidant potential of Pongamia pinnata in wistar rats, J. Tradit. Complementary Med. 7 (1) (2017) 79–85.
[9] M. Jarrahi, An experimental study of the effects of Matricaria chamomilla extract on cutaneous burn wound healing in albino rats, Nat. Prod. Res. 22 (5) (2008) 422–427.
[10] B.S. Nayak, S.S. Raju, A.V. Rao, Wound healing activity of Matricaria recutita L. extract, J. Wound Care 16 (2007) 298–302.
[11] D.L. Mathieu, J. C, F. Wattel, Non-healing wounds, in: D.E. Mathieu (Ed.), Handbook on Hyperbaric Medicine, Springer, Netherlands, 2006, pp. 401–427.
[12] R.H. Müller, M. Radtke, S.A. Wissing, Solid lipid nanoparticles (SLN) and nanostructured lipid carriers (NLC) in cosmetic and dermatological preparations, Adv. Drug Deliv. Rev. 54 (2002) 131–155.
[13] A. Angelova, V.M. Garamus, B. Angelov, Z. Tian, Y. Li, A. Zou, Advances in structural design of lipid-based nanoparticle carriers for delivery of macromolecular drugs, phytochemicals and anti-tumor agents, Adv. Colloid Interface Sci. 249 (2017) 331–345.
[14] Y. Chen, A. Angelova, B. Angelov, M. Drechsler, V.M. Garamus, R. Willumeit-Römer, A. Zou, Sterically stabilized spongosomes for multidrug delivery of anticancer nanomedicines, J. Mater. Chem. B 3 (2015) 7734–7744.
[15] L.P.B. Guerzoni, V. Nicolas, A. Angelova, In vitro modulation of TrkB receptor signaling upon sequential delivery of curcumin-DHA loaded carriers towards promoting neuronal survival, Pharmaceut. Res. 34 (2017) 492–505.
[16] G. Gainza, M. Pastor, J.J. Aguirre, S. Villullas, J.L. Pedraz, R.M. Hernandez, et al., A novel strategy for the treatment of chronic wounds based on the topical administration of rhEGF-loaded lipid nanoparticles: in vitro bioactivity and in vivo effectiveness in healing-impaired db/db mice, J. Contr. Release 185 (2014) 51–61.
[17] I. Garcia-Orue, G. Gainza, C. Girbau, R. Alonso, J.J. Aguirre, J.L. Pedraz, et al., LL37 loaded nanostructured lipid carriers (NLC): a new strategy for the topical treatment of chronic wounds, Eur. J. Pharm. Biopharm. 108 (2016) 310–316.
[18] E. Esposito, C. Sticozzi, L. Ravani, M. Drechsler, X.M. Muresan, F. Cervellati, R. Cortesi, G. Valacchi, Effect of new curcumin-containing nanostructured lipid dispersions on human keratinocytes proliferative responses, Exp. Dermatol. 24 (2015) 449–454.
[19] H.A. Gad, A.O. Kamel, O.M. Ezzat, H.F. El Dessouky, O.A. Sammour, Doxycycline hydrochloride-metronidazole solid lipid microparticles gels for treatment of periodontitis: development, in-vitro and in-vivo clinical evaluation, Expert Opin. Drug Deliv. 14 (2017) 1241–1251.
[20] G. Gainza, W.S. Chu, R.H. Guy, J.L. Pedraz, R.M. Hernandez, B. Delgado-Charro,

et al., Development and in vitro evaluation of lipid nanoparticle-based dressings for topical treatment of chronic wounds, Int. J. Pharm. 490 (1) (2015) 404–411.
[21] H.A. Gad, M.A. El-Nabarawi, S.S. Abd el-Hady, Formulation and evaluation of secnidazole or doxycycline dento-oral gels, Drug Dev. Ind. Pharm. 34 (2008) 1356–1367.
[22] H.B. Waynforth, P.A. Flecnell, Anaesthesia and Postoperative Care, Experimental and Surgical Technique in the Rat, second ed., Academic Press Inc., London, 1992.
[23] H.L. Walker, A.D. Masson, A standard animal burn, J. Trauma 8 (6) (1968) 1049–1051.
[24] G.L. Humason, Animal Tissue Techniques, third ed., W.H. Freeman Company, San Francisco, 1972.
[25] E. Gurr, A Practical Manual of Medical and Biological Staining Techniques, Interscience, New York, 1956.
[26] U.K. Sinha, L.A. Gallagher, Effects of steel scalpel, ultrasonic scalpel, CO_2 laser, and monopolar and bipolar electro surgery on wound healing in Guinea pig oral mucosa, Laryngoscope 113 (2003) 228–236.
[27] M.H. Khalil, J.F. Marcelletti, L.R. Katz, D.H. Katz, L.E. Pope, Topical application of docosanol- or stearic acid-containing creams reduces severity of phenol burn wounds in mice, Contact Dermatitis 43 (2) (2000) 79–81.
[28] F.Q. Hu, S.P. Jiang, Y.Z. Du, H. Yuan, Y.Q. Ye, S. Zeng, et al., Preparation and characterization of stearic acid nanostructured lipid carriers by solvent diffusion method in an aqueous system, Colloids Surf., B 45 (3–4) (2005) 167–173.
[29] L.J. Jia, D.R. Zhang, Z.Y. Li, F.F. Feng, Y.C. Wang, W.T. Dai, et al., Preparation and characterization of silybin-loaded nanostructured lipid carriers, Drug Deliv. 17 (1) (2010) 11–18.
[30] C. Braem, T. Blaschke, G. Panek-Minkin, W. Herrmann, P. Schlupp, T. Paepenmüller, et al., Interaction of drug molecules with carrier systems as studied by parelectric spectroscopy and electron spin resonance, J. Contr. Release 119 (1) (2007) 128–135.
[31] R.H. Müller, R.D. Petersen, A. Hommoss, J. Pardeike, et al., Nanostructured lipid carriers (NLC) in cosmetic dermal products, Adv. Drug Deliv. Rev. 59 (6) (2007) 522–530.
[32] S.A. Wissing, R.H. Müller, The influence of the crystallinity of lipid nanoparticles on their occlusive properties, Int. J. Pharm. 242 (1) (2002) 377–379.
[33] E.B. Souto, S.A. Wissing, C.M. Barbosa, R.H. Müller, Development of a controlled release formulation based on SLN and NLC for topical clotrimazole delivery, Int. J. Pharm. 278 (1) (2004) 71–77.
[34] S. Das, W.K. Ng, R.B.H. Tan RBH, Are nanostructured lipid carriers (NLCs) better than solid lipid nanoparticles (SLNs): development, characterizations and comparative evaluations of clotrimazole-loaded SLNs and NLCs? Eur. J. Pharm. Sci. 47 (2012) 139–151.
[35] V. Teeranachaideekul, P. Boonme, E.B. Souto, R.H. Müller, V.B. Junyaprasert, et al., Influence of oil content on physicochemical properties and skin distribution of Nile red-loaded NLC, J. Contr. Release 128 (2008) 134–141.
[36] R. Avallone, P. Zanoli, G. Puia, M. Kleinschnitz, P. Schreier, M. Baraldi, Pharmacological profile of apigenin, a flavonoid isolated from *Matricaria chamomilla*, Biochem. Pharmacol. 59 (2000) 1387–1394.
[37] M.D. Martins, M.M. Marques, S.K. Bussadori, M.A.T. Martins, V.C.S. Pavesi, R.A.M. Ferrari, K.P.S. Fernandes, Comparative analysis between *Chamomilla recutita* and corticosteroids on wound healing. An *in vitro* and *in vivo* study, Phytother Res. 23 (2009) 274–278.
[38] J.K. Tessmar, A.M. Göpferich, Matrices and scaffolds for protein delivery in tissue engineering, Adv. Drug Deliv. Rev. 59 (2007) 274–291.
[39] M. Schäfer-Korting, W. Mehnert, H.C. Korting, Lipid nanoparticles for improved topical application of drugs for skin diseases, Adv. Drug Deliv. Rev. 59 (6) (2007) 427–443.
[40] C.S.J. Campbell, L.R. Contreras-Rojas, M.B. Delgado-Charro, R.H. Guy, Objective assessment of nanoparticle disposition in mammalian skin after topical exposure, J. Contr. Release 162 (2012) 201–207.
[41] A.E. Krausz, B.L. Adler, V. Cabral, M. Navati, J. Doerner, Charafeddine, D. Chandra, H. Liang, L. Gunther, A. Clendaniel, S. Harper, J.M. Friedman, J.D. Nosanchuk, A.J. Friedman, Curcumin-encapsulated nanoparticles as innovative antimicrobial and wound healing agent, Nanomed. Nanotechnol. Biol. Med. 9 (4) (2014) 1–13.
[42] T.K. Lin, L. Zhong, J.L. Santiago, Anti-inflammatory and skin barrier repair effects of topical application of some plant oils, Int. J. Mol. Sci. 19 (70) (2018) 1–21.
[43] M.M. Domingues, M.M. Martins, B.S. Kalil, M.M.A. Trevizani, P.V.C. Santos, M.F.R. Agnelli, et al., Comparative analysis between Chamomilla recutita and corticosteroids on wound healing. An in vitro and in vivo study, Phytother Res. 23 (2) (2009) 274–278.
[44] R. Lobmann, C. Zemlin, M. Motzkau, K. Reschke, H. Lehnert, Expression of matrix metalloproteinases and growth factors in diabetic foot wounds treated with a protease absorbent dressing, J. Diabet. Complicat. 20 (5) (2006) 329–335.
[45] S. Patel, A. Maheshwari, A. Chandra, Biomarkers for wound healing and their evaluation, Wound Care 25 (1) (2016) 46–55.